Available online at www.sciencedirect.com

SCIENCE DIRECT®

Journal of Volcanology and Geothermal Research 142 (2005) 105–118

Journal of volcanology and geothermal research

www.elsevier.com/locate/jvolgeores

Glass transition temperatures of natural hydrous melts: a relationship with shear viscosity and implications for the welding process

D. Giordano[a,b,*], A.R.L. Nichols[b], D.B. Dingwell[b]

[a]*Department of Geological Sciences, Terza Università degli Studi di Roma, Italy*
[b]*Department of Earth and Environmental Sciences, University of Munich, Germany*

Received 22 October 2003; accepted 8 October 2004

Abstract

Glass transition temperatures (T_g) have been determined for natural multicomponent melts using differential scanning calorimetry. Trachytic, dacitic, phonolitic and basaltic base compositions have been analysed over a range of water contents up to 3.75 wt.%. For each sample T_g has been obtained over a range of cooling/heating rates using the extrapolated onset and the peak temperatures in heat capacity–temperature curves. T_g of all compositions are strongly reduced by increasing water content, particularly for the first 1 wt.% added. Base composition also has an effect, with the lowest T_g occurring in the peralkaline phonolite suite. For all samples a clear dependence on the cooling/heating rate has been recorded. These results have been compared with rheological investigations on the same samples. On the basis of the equivalence of the shear and enthalpic relaxation process timescales we provide a method to predict the shear viscosity at the glass transition for all the melts investigated in this study, both dry and hydrous. Our determinations of T_g provide a lower limit for the time–temperature envelope that gives rise to densely welded deposits and constraints on their emplacement temperature. Furthermore, by using the viscosity values predicted at the glass transition, we suggest that welding processes may occur over timescales on the order of tens of seconds to tens of minutes at T_g.

Keywords: glass transition; calorimetry; viscosity; welding temperatures

1. Introduction

Welding of hot primary volcanic deposits (e.g. ignimbrites, spatter-rich flows and fallout deposits) occurs due to the presence of glassy material (pumice and bubble wall shards) in the deposits (Smith, 1960a,b; Ross and Smith, 1961; Sparks and Wright,

* Corresponding author. Department of Geological Sciences, Terza Università degli Studi di Roma, Italy. Fax: +1 604 822 6088.
E-mail addresses: dgiordan@uniroma3.it, dgiordano@eos.ubc.ca (D. Giordano).

0377-0273/$ - see front matter © 2004 Elsevier B.V. All rights reserved.
doi:10.1016/j.jvolgeores.2004.10.015

1979; Sparks et al., 1999; Gottsmann and Dingwell, 2001, 2002). The process varies in extent from limited adhesion or sintering of fragments at their points of contact, to more intense welding involving viscous deformation of clasts and compaction of the deposit. In extreme cases, an almost complete homogenisation of the glass and obliteration of the original vitroclastic texture can be achieved (Ross and Smith, 1961; Branney et al., 1992; Gottsmann and Dingwell, 2001, 2002). In such cases where complete homogenisation occurs it may be impossible to recover the welding history. The welding process is fundamentally possible when the viscosity of the fragments is sufficiently low to permit significant deformation and sintering under the time–temperature paths provided by the cooling history of the deposit under the available lithostatic load. Historically, temperature has been invoked as the main factor controlling viscosity of pyroclasts at a given temperature (see Ross and Smith, 1961 for a review). Under such a model, the "minimum welding temperature" is the temperature at which the particles attain the highest viscosity during the welding process, effectively the temperature at which the dense welding process ceases during cooling. The minimum welding temperature of rhyolitic material has been determined, based on experimental and field constraints, to range from 600 to 775 °C (Boyd and Kennedy, 1951; Biewirth, 1982; Kamata et al., 1993).

Experimental initiatives have, in the past decade, greatly improved the description of the viscosity of volcanic "glasses" just above the glass transition (e.g. Hess and Dingwell, 1996). Dilatometric investigations of melt viscosity in this so-called "welding interval" (e.g. Giordano et al., 2000) have begun to provide a quantitative picture of the variation of viscosity with bulk composition, temperature and with trace water content (e.g. Gottsmann et al., 2002; Hess et al., 2001). Early observations of the strong effect of volatiles, and especially water, on the viscosity in this high-viscosity range (Friedman et al., 1963) have been confirmed by more recent studies (e.g. Hess and Dingwell, 1996; Giordano et al., 2004). This has led to the general realisation that even for largely degassed volcanic fragments cooling in near surface deposits, the influence of both temperature and water content on the viscosity must be incorporated in any general parameterisation of the viscosity of volcanic glasses in the welding interval.

Comparisons of calorimetric and dilatometric determinations of the glass transition interval have demonstrated clearly that calorimetric glass transition temperature data can be converted quantitatively into viscosity data (Stevenson et al., 1995; Gottsmann et al., 2002). Due to the relative speed and efficiency of determining the glass transition calorimetrically, it is especially well-suited to quantifying viscosity in materials where the stability and size of the samples challenge viscometry by conventional means (e.g. Dingwell et al., 2004). Here, the calorimetric determination of the glass transition temperature, and through it the viscosity at the glass transition, has been performed on a suite of multicomponent volcanic glasses with variable water contents. This information provides a quantitative scaling of the deformability of volcanic glasses via viscous flow. The multicomponent composition, water content and temperature, or deformability are quantitatively linked to provide a parameterisation of the ability of volcanic glasses to weld under given thermal and loading histories.

2. Background

2.1. A characteristic temperature for welding?

As it is glass particles within a volcanic deposit that undergo welding, one of the most important factors governing the welding process is the glass transition. The importance of this temperature interval is often not realised in welding literature. It is as important as emplacement temperature, crystallisation temperature and minimum welding temperature.

If, for example, a volcanic material is emplaced at high temperatures, well above the minimum welding temperature, and closer to their crystallisation temperature, syn- to post-emplacement crystallisation may occur, possibly preventing welding. Such a scenario is the most common fate of subaerial basalts, because crystallization is relatively rapid, pre-empting the welding process. On the other hand, more siliceous materials, such as rhyolites and phonolites, have emplacement temperatures that are closer to their minimum welding temperature and crystal growth rates are much slower. This increases the likelihood of

deposits with inhibited crystallization, and so preserving glass. Thus, the relationships between these characteristic temperatures for each material, combined with the rates of crystallisation and cooling, determine whether the deposit crystallises or whether welding occurs and a glass is preserved.

At this point the minimum welding temperature is still undefined. Indeed, every time a different experimental technique is used to directly determine the welding rate under given temperature–load pressure conditions a different definition is provided. The definition is empirical in nature and, therefore, not unique to constrain. Several values are given for different samples at different conditions (e.g. Ross and Smith, 1961; Schmincke, 1974; Ragan and Sheridan, 1972; Miller and Riehle, 1994; Riehle et al., 1995). What is clear is that the minimum welding temperature is a temperature above which a material can deform in a ductile manner for a given thermal and loading history. Given the central role of viscous deformation in welding, this minimum welding temperature, will, for a given loading and thermal history, scale to the glass transition temperature. It can thus be constrained as a function of multicomponent melt chemistry and water content. The only proviso for this assumption is that the temperature dependence of the viscosity near the glass transition is roughly similar for all compositions. The great advantage of the scalability of the minimum welding temperature to the glass transition temperature is that the glass transition is easily quantifiable in terms of cooling history and composition using a number of experimental methods (e.g. Scherer, 1984; Stevenson et al., 1995; Gottsmann et al., 2002).

2.2. The glass transition interval

The glass transition (T_g) is a kinetic boundary between a liquid-like (viscous) and solid-like (elastic) mechanical response to an applied stress (e.g. Dingwell and Webb, 1990). Above the glass transition glassy particles will deform viscously, permitting welding, whereas below T_g, the glass will respond to stresses in an elastic manner, thereby making welding impossible. The temperature interval across which the glass transition is observed depends on composition, thermal history and, experimentally, upon the timescale of the investigative method. It is the kinetic essence of the glass transition that it is representable by a time–temperature curve, not a single temperature. Thus it may be crossed from the liquid to the glassy field either in temperature (e.g. by cooling at a constant load) or in time through decreasing the timescale of deformation (e.g. by increased loading at constant temperature). Either way, passing through the glass transition into the glassy field will arrest the welding process.

The glass transition may be defined using many physical properties. One of the simplest descriptions, and one which immediately reveals the link to viscosity and thus viscous deformation and welding, is Maxwell's (1867) law of linear viscoelasticity:

$$\tau = \frac{\eta_N}{G_\infty} \tag{1}$$

where G_∞ is the shear (rigidity) modulus (Pa) at infinite frequency, η_N is the Newtonian shear viscosity of the liquid (Pa s) and τ is the relaxation time (s). The crossing of the glass transition with cooling results from the exponential decrease with temperature of the self-diffusivity of Si and other components in the liquid (Dingwell and Webb, 1989). The effective freezing out of the self-diffusion in this manner affects the kinetics of a host of processes (e.g. viscous flow, growth and nucleation of crystals and bubbles). Although crystallisation has been avoided, the liquid is effectively "frozen" to a glass.

Due to the thermally activated nature of the structural relaxation, Newtonian viscosities across the glass transition vary with cooling history. In fact, this feature has been used to map thermal histories of natural volcanic glasses in many deposits, some of them welded (Wilding et al., 1995, 1996, 2000; Gottsmann and Dingwell, 2001, 2002). In doing so, it has been demonstrated that natural cooling rates may vary by up to 5 orders of magnitude at a single eruptive centre. Cooling rates have been demonstrated to be linearly proportional to relaxation times (Scherer, 1984; Dingwell and Webb, 1990; Dingwell, 1996): i.e. the slower the cooling rate, the longer the effective relaxation time associated with it, and the lower the glass transition temperature. This allows a higher equilibrium viscosity to be reached during slower cooling (e.g. Scherer, 1984; Stevenson et al., 1995; Gottsmann et al., 2002).

In this study, we have performed calorimetric measurements across the glass transition for several base compositions (trachytic, dacitic, phonolitic and basaltic) containing a range of water contents. From the resulting data we have been able to define single temperatures (T_g), at the low-temperature onset of the glass transition and within the glass transition interval, to be used as two scaling temperatures for minimum welding temperatures. Using viscosity–temperature relationships defined for the same samples we have been able to calculate the viscosity at these temperatures. Then using Eq. (1) we have calculated the relaxation time (τ) for each of the glass compositions at T_g.

3. Methods

3.1. Sample selection and preparation

The samples investigated were obtained from natural samples and are trachytic (IGC; Campanian Ignimbrite, and MNV; Monte Nuovo, both from the Phlegrean Fields), dacitic (UNZ; from Unzen, Kyushu), phonolitic (Td_ph; from Teide, Tenerife) and basaltic (ETN; from Etna, Sicily) in composition (Table 1).

Table 1
Composition (wt.%) of the analysed liquids from Teide (Td_ph—phonolite), Etna (ETN—basalt), Campanian Ignimbrite (IGC—trachyte), Monte Nuovo (MNV—trachyte) and Unzen (UNZ—dacite)

	Td_ph[a]	ETN[b]	IGC[c]	MNV[c]	UNZ[c]
SiO_2	60.46	47.03	60.74	63.88	66.00
Al_2O_3	18.81	16.28	19.22	17.10	15.23
FeO_{tot}	3.31		3.37	2.90	4.08
FeO	–	3.34	–	–	–
Fe_2O_3	–	7.54	–	–	–
TiO_2	0.56	1.61	0.27	0.31	0.36
MnO	0.20	0.20	0.18	0.13	0.10
MgO	0.36	5.17	0.28	0.24	2.21
CaO	0.67	10.47	2.11	1.82	5.01
Na_2O	9.76	3.75	5.28	5.67	3.84
K_2O	5.45	1.94	6.32	6.82	2.16
P_2O_5	0.06	0.59	0.06	0.05	0.14

[a] Giordano et al. (2000).
[b] Giordano and Dingwell (2003a).
[c] Giordano et al., (2004); Giordano and Dingwell (2003b).

In order to obtain crystal-free and bubble-free glasses for viscometry and calorimetry the glassy matrix (MNV, IGC, Td_ph) or total rock (UNZ, ETN) of the samples were melted and then quenched. These gave the base compositions in a virtually anhydrous state with water contents below 500 ppm. About 100 g batches of each sample were loaded separately into a Deltech furnace and melted at 1300 to 1600 °C (depending on composition) and stirred for several hours. After inspection of the stirring spindle revealed that the melts were physically homogeneous, their viscosity was measured (see below) and then they were removed from the furnace and quenched in air, either within the crucible, or by pouring on to a steel plate. Cylinders, approximately 6 mm in diameter, were cored from the glasses and cut into disks 2 to 3 mm thick. These were then doubly polished, dried and stored in a dessicator until further use.

3.2. Synthesis of hydrous samples

Hydrous samples were prepared from each of the base (anhydrous) compositions using a piston cylinder apparatus at 10 kbar and temperatures up to 1600 °C. The homogenised glasses from the high temperature viscometry were powdered and loaded together with known amounts of doubly distilled water into platinum capsules, which were then sealed by arc welding. To check that water was unable to leak from the capsules they were weighed before and after being placed in an oven at 110 °C for at least an hour. No weight difference was observed. The heating also ensured that the water was homogeneously distributed within the capsules. For each base composition three to four hydrous samples containing different amounts of water were synthesised and then rapidly quenched. This resulted in a suite of samples with a range of water contents for each composition (see Table 2). Hydrous samples were doubly polished into sections about 1 mm thick and stored in a dessicator until further use. Fourier-transform infrared (FTIR) spectroscopy was used to confirm the homogeneous nature of the distribution of water and to measure its concentration before and after viscosity determination. The Karl–Fischer titration (KFT) technique was used to determine the absolute water content of each sample.

Table 2
Glass transition temperatures (T_g) determined for each sample using differential scanning calorimetry

Sample	Composition	H_2O content	T_g^{peak} (°C±1) cooling/heating rate (K/min)					T_g^{onset} (°C±2.5) cooling/heating rate (K/min)				
			20	15	10	5	1	20	15	10	5	1
IGC	Trachyte	0.04	788	776	768	741		731	722	714	687	
812		0.81	595	587	580	562		532	528	521	527	
IGC2		1.52	545	535	527	512		489	483	478	470	
IGC1		2.01	504	496	488	478		447	442	439	419	
ETN	Basalt	0.02	739	733	726	716		692	688	681	673	
801		0.64	616	615	611	609		571	567	563	556	
800		1.13	580	579	576	568		515	509	503	500	
BET 1–3		1.64	560	557	550			505	499	496		
802		2.31	531	530	516			459	457	459		
MNV	Trachyte	0.03	721		710			658		636		
804		1.00	618	606	584	541		554	542	527	488	
806		1.39	522	521	517	506		465	464	454	447	
805		2.41	478	473	461	452		424	415	414	405	
Td_ph	Phonolite	0.03	670	665	656	648	621	610	603	599	590	548
706		0.85	522	516	509	501		467	464	458	453	
705		0.95	505	500	492	482		452	449	444	439	
704		2.10	456	451	446	434		402	399	394	388	
702		3.75	403	398	392	382		354	348	343	340	
UNZ	Dacite	0.05	745		731	719		688		676	668	
U4		1.37		587	575	563			534	528	519	
U3		1.60	562	554	548	534		507	506	500	493	
U2		1.98	546	539	533	522		497	491	487	481	

These have been determined using matching cooling and heating rates. The methods to define T_g^{peak} and T_g^{onset} are shown in Fig. 1. The uncertainty for T_g^{peak} is based on the reproducibility of the calorimetric apparatus. The uncertainty estimated for determining T_g^{onset} is greater because it relies on extrapolations from the calorimetric trace (Fig. 1).

3.3. Viscometry

Low-viscosity measurements, between 10^2 and 10^5 Pa s, were obtained using the concentric cylinder system and methods described by Dingwell (1991). These were performed on the anhydrous samples, directly after homogenisation, in the Deltech furnace using a Brookfield DVIII (full-scale torque= 5.75×10^{-1} N m) viscometer head and a $Pt_{80}Rh_{20}$ low-viscosity spindle described by Dingwell and Virgo (1988). The viscosity was determined in steps of decreasing temperature with a final measurement at the highest temperature to check for any drift during the measurements. The viscosity standard, DGG-1, was used to calibrate the system and the viscosities are accurate to ±5%.

Viscosities in the range of $10^{8.5}$ to 10^{12} Pa s were measured using the micropenetration method. This involves determining the rate at which a hemispherical Ir-indenter moves into a melt surface under a fixed load. One of the main advantages of this technique is the small amount of sample (less than 10 mg) required. The measurements were performed using a Bähr 802 V vertical push-rod dilatometer and consisted of a heating phase, a subsequent relaxation phase and a run phase during which the indenter was left free to penetrate the surface of the sample. After completion of the measurement the sample was cooled at a fixed rate. Oxidation of the sample was prevented throughout the measurements by directing a flow of Ar (3 l/min) across the sample. Measurements of both anhydrous and hydrous samples were performed over a range of temperatures up to about 100 °C above their glass transition temperatures.

In order to check for possible loss of water during micropenetration, water contents were determined by FTIR spectroscopy and Karl–Fischer titration before and after the measurements. In addition, to check whether bubble nucleation or water exsolution possibly affecting viscometry had occurred during micropenetration, duplicate viscosity measurements on single samples at the same temperature were performed. The

analyses revealed that there was no evidence for loss of water (see also details in Giordano et al., 2004).

3.4. Calorimetry

In order to obtain the variation of specific heat capacity (c_p) with temperature across the glass transition calorimetric measurements were performed using a differential scanning calorimeter (Netzsch ® DSC 404 C Pegasus). The first stage of each measurement was to obtain a baseline, where the heat flow from two identical empty Pt–Rh crucibles (6 mm in diameter) was measured. The DSC was then calibrated by measuring the heat flow of a single sapphire crystal placed in one of the crucibles against an empty crucible. Finally, the heat flow of doubly polished disks of sample were measured against the empty crucible. The mass of sample matched, as closely as possible, that of the sapphire standard (either 27.77 or 53.85 mg). All measurements were performed with the same two crucibles and under a constant flow of Ar gas. The c_p data were calculated using all the heat flow data, the sample masses and the known c_p of the sapphire standard.

Initially the sample was heated from 40 °C across the glass transition at a rate of 5 K/min. Then the same sample was subjected to a series of measurements during which cooling rates of 20, 15, 10, 5, and, in the case of one sample (Teide phonolite), 1 K/min were matched by subsequent heating rates. In each case, in order to allow complete structural relaxation, the samples were heated above the glass transition into the super-cooled liquid field (Fig. 1). However, the time spent above the glass transition was kept at a minimum to prevent the loss of water. Therefore, for each sample a series of c_p curves were determined from which T_g (a single temperature) could be defined (rather than a temperature interval) in relation to cooling/heating rate.

Two methods were used to define T_g from the c_p data. Firstly, the temperature at which the peak in the c_p curve occurs was used to define the T_g^{peak} (Fig. 1). Also the temperature at which the extrapolated onset of the rapid increase of c_p occurred was used to define the T_g^{onset} (as described by Moynihan, 1995) (Fig. 1). The reason for defining T_g in these two ways is that although the T_g^{onset} marks the beginning of the relaxation process, and is therefore of more interest, the T_g^{peak} can be defined with more certainty, as it does not rely on extrapolations (Fig. 1). We use both as scaling temperatures for minimum welding temperatures.

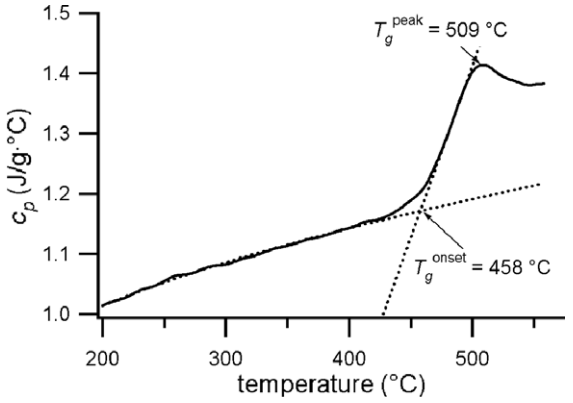

Fig. 1. Variation of specific heat capacity (c_p) with temperature across the glass transition for a sample containing 0.85 wt.% water from the Td_ph compositional suite. The cooling and heating rates used to generate these data are 10 K/min. The glass transition is defined as the temperature interval between the temperature at which the c_p curve deviates from the glassy state (fitted by the Maier–Kelley curve equation $c_p=a+bT+cT^{-2}$) and the temperature at which c_p achieves a constant value (indicating entry into the super-cooled liquid field) at temperatures above the c_p peak. Glass transition temperatures (T_g) have been defined in two ways: (i) the temperature at which the maximum in c_p across the glass transition occurs (T_g^{peak}); (ii) the temperature where the extrapolations of the fit of the glassy state and the sudden increase in c_p (denoted by dotted lines) intersect (T_g^{onset}). The uncertainty in defining T_g^{peak} is ±1 °C, whereas due to the fact that T_g^{onset} is defined by the intersection of two extrapolations its uncertainty is somewhat larger at ±2.5 °C.

There is the possibility that water could have been lost from the hydrous samples across the glass transition and in the super-cooled liquid field. However, after carefully examining and weighing the samples after each measurement in the series we are confident that this did not occur. Furthermore, we repeated single measurements on the same sample and obtained c_p curves that were within the reproducibility of the apparatus.

4. Results and discussion

4.1. Viscosities

The measured viscosities are reported in Giordano et al. (2000), Giordano and Dingwell (2003a) and

Giordano et al. (2004) for Td_ph, ETN, IGC and MNV samples and in Table 3 for UNZ. Fig. 2 shows, as examples, the variation of viscosity versus reciprocal temperature for the MNV and IGC samples (from Giordano et al., 2004). For all anhydrous compositions, viscosity clearly exhibits a non-Arrhenian relationship with temperature. The viscosities measured for anhydrous and hydrous samples can be parameterised by the following empirical Vogel–Fulcher–Tammann (VFT) equation, modified to take into account the effect of water (e.g. Giordano et al., 2000):

$$\log_{10}\eta = [a_1 + a_2\ln(H_2O)] + \{[b_1 + b_2H_2O] / [T - (c_1 + c_2\ln(H_2O))]\} \quad (2)$$

where a, b and c are adjustable parameters (listed for each composition in Table 4), H_2O is the water content (in wt.%) and T is temperature (in K). This equation reproduces the measured viscosities within the experimental errors. Even though our study has investigated the relationships between the calorimetric and rheological properties across the glass transition region, i.e. in the low-temperature/high-viscosity interval between $10^{8.5}$ and 10^{12} Pa s, the high-temperature data for anhydrous samples were included to calibrate the adjustable parameters, a, b and c in Eq. (2). This allowed a more accurate description of all the measured viscosities. This equation was then used to calculate viscosities at T_g defined using the c_p data (Fig. 1).

Table 3
Measured viscosities for the UNZ dacite sample

H_2O (wt.%)	T_{meas} (°C)	$\log_{10}\eta$ (Pa s)
0.04	1471	2.09
0.04	1446	2.21
0.04	1422	2.34
0.04	1397	2.48
0.04	1373	2.62
0.04	1348	2.76
0.04	1323	2.92
0.04	1299	3.08
0.04	1274	3.25
0.04	1249	3.43
0.04	1225	3.61
0.04	1200	3.80
0.04	1176	4.00
0.04	1151	4.21
0.04	1126	4.44
0.04	1102	4.66
0.04	761.0	10.50
0.04	784.7	9.85
0.04	801.0	9.28
0.04	818.0	8.91
1.31	588.9	10.56
1.31	561.9	11.18
1.64	498.9	11.95
1.64	534.8	11.12
1.64	535.3	10.93
1.64	565.4	9.86
1.98	530.8	10.48
1.98	541.9	9.99
1.98	560.4	9.63

The water content is reported in wt.%. For the anhydrous sample we assumed a water content of 0.04 wt.%, in accordance with the amount of water estimated in virtually dry liquids by Ohlhorst et al. (2001).

The isothermal variation of viscosity with water content is shown in Fig. 3 at temperatures appropriate to welding processes for each investigated composition. The first 1 wt.% of water added strongly decreases the viscosity, while with further addition the effect levels off. This agrees with previous studies on a range of liquid compositions (e.g. Richet et al., 1996; Whittington et al., 2000, 2001; Giordano et al., 2004).

4.2. Glass transition temperatures (T_g)

T_g^{peak} and T_g^{onset} are listed in Table 2 and their variation with water content in each compositional suite is shown in Figs. 4 and 5. Fig. 4 shows the T_g^{peak} and T_g^{onset} for different cooling/heating rates. This confirms the observation of Scherer (1984), Stevenson et al. (1995) and Gottsmann et al. (2002) that T_g depends on the thermal history. Therefore one must be very careful that when quoting T_g that the cooling and heating rates are given. Furthermore the way in which T_g is defined should also be provided, as the specific value of T_g will depend on this.

T_g appears to be strongly dependent on water content, decreasing as water content increases. For clarity we now discuss T_g measured using a cooling/heating rate of 10 K/min (Fig. 5), because we have successfully measured c_p in all of our samples at this cooling/heating rate (Table 2). Across the range of water contents analysed here water seems to have the largest effect on the IGC composition, the addition of 2.01 wt.% decreases T_g^{peak} by 280 °C and T_g^{onset} by 275 °C. The smallest effect is on the UNZ composition where the addition of 1.98 wt.% reduces T_g^{peak} by 198 °C and T_g^{onset} by 189 °C. For all compositions the

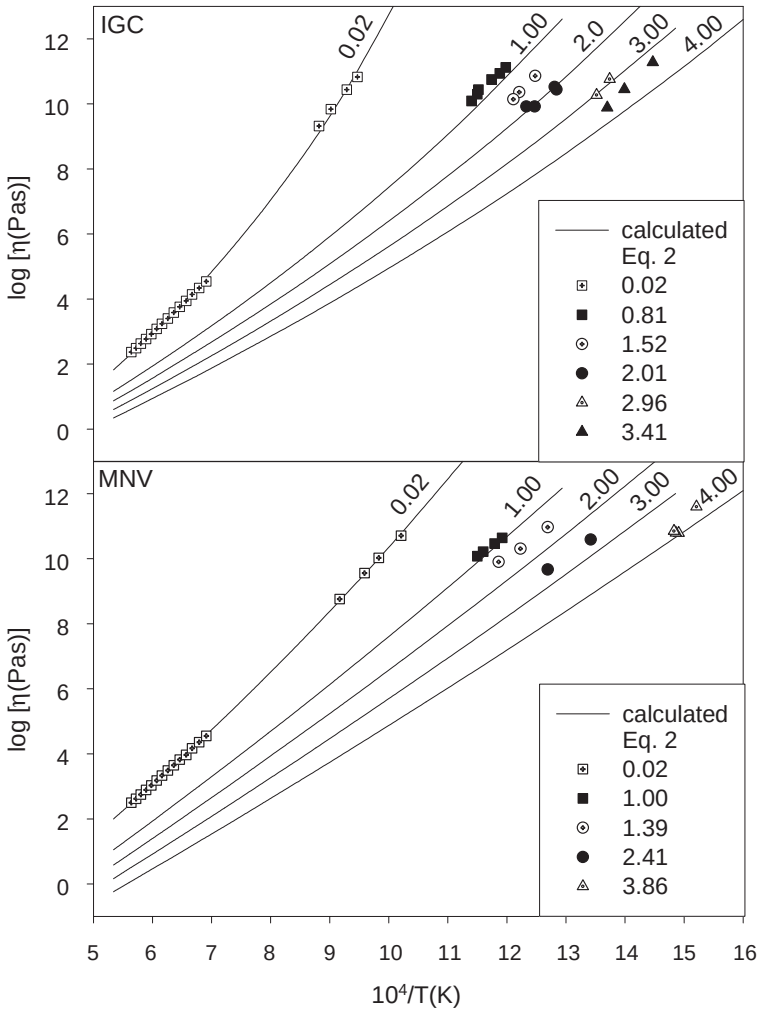

Fig. 2. Relationship between measured viscosity and temperature (expressed as 10^4/T) for the Campanian Ignimbrite (IGC) and the Monte Nuovo (MNV) samples. Each symbol refers to measured viscosity at the water contents given in the legend. The lines show the viscosity calculated at the water contents indicated. From Giordano et al. (2004).

largest effect is in the initial 1 wt.% of water added causing decreases in T_g^{peak} of 202, 141, 126, 158 and 112 °C for the IGC, ETN, MNV, Td_ph and UNZ compositional suites respectively. Addition of a further 1 wt.% of water causes decreases of only 77, 53, 100, 47 and 87 °C respectively in T_g^{peak}.

The Td_ph suite has the lowest T_g of any of the samples over the entire range of water contents investigated. T_g^{peak} with cooling/heating rates of 10 K/min are 112 to 54, 121 to 68, 81 to 33, and 85 °C lower than any other composition at 0, 1, 2 and 3 wt.% water respectively. This is consistent with previous viscosity measurements on related compositions by Giordano et al. (2000) and Whittington et al. (2001). It is difficult to determine the structural reason for this. One might expect there to be a straightforward relationship between T_g and the polymerisation in the melt. Using the ratio of non-bridging oxygens to tetrahedral cations (NBO/T) this is not seen to be the case (Giordano and Dingwell, 2003c). As discussed in Giordano and Dingwell (2003b) in terms of viscosity, this may be due to either uncertainty in quantifying NBO/T, or the fact that the algebraic formulation of NBO/T

Table 4
Calibrated parameters for Eq. (2)

Sample	a_1	a_2	b_1	b_2	c_1	c_2	Average standard error[a]
Td_ph	−5.900	−0.286	10775	−394.8	148.7	−21.65	0.115
ETN	−4.643	–	5812	−427.0	499.3	−28.74	0.226
MNV	−5.863	−0.051	12747	−673.5	103.4	−25.99	0.118
IGC	−4.415	0.098	9243	−428.1	255.3	−55.15	0.097
UNZ	−1.731	0.624	7995	−1257.2	344.5	−37.57	0.190

Listed values allow the calculation of $\log_{10}$ of viscosity in units of Pa s when temperature is in K and water content is in wt.%.
[a] Average standard errors are calculated by fitting the experimental data to Eq. (2).

does not directly reflect the polymerisation in the melt, or that polymerisation is not a critical controlling factor of T_g. There are other ways in which polymerisation in the melt can be expressed (see for instance Whittington et al., 2001; Romano et al., 2003; Giordano et al., 2004 for more details). However, even in terms of the structure modifying cation (SM) parameter (see Giordano and Dingwell, 2003b for definition), for example, there is no simple relationship (Romano et al., 2003; Giordano et al., 2004). Although the high alkaline content in the Td_ph composition could be responsible for the low T_g of this suite, there is no direct relationship between our T_g data and alkaline content.

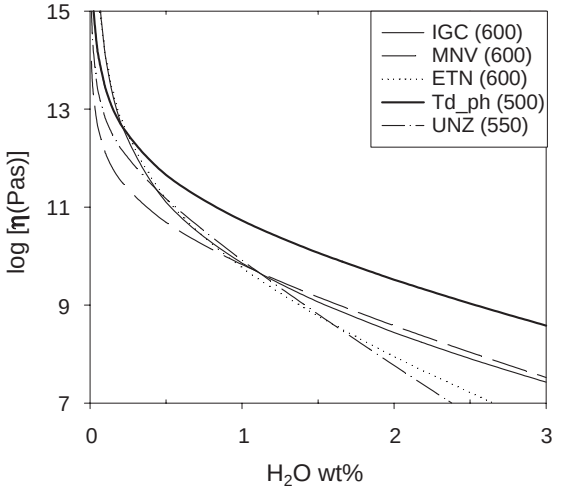

Fig. 3. Variation of viscosity with water content at isothermal temperatures (in °C) appropriate to the welding conditions of the different magmatic liquids investigated. The curves are calculated on the basis of Eq. (2).

4.3. Viscosities at glass transition temperatures (η_{T_g})

Traditionally, in terms of viscosity, T_g is defined as the temperature at which the viscosity is 10^{12} Pa s. However, as confirmed by the calorimetry data presented here, T_g depends upon the cooling and heating rate and of course the way in which T_g is graphically defined.

Using Eq. (2) we have calculated viscosities at T_g^{peak} and T_g^{onset}, defined using cooling/heating rates of 10 K/min, for all compositions and water contents (Fig. 6). Effectively at T_g^{peak} or T_g^{onset} the viscosity changes little, irrespective of base composition or water content. This is a strong confirmation of the validity of Eq. (1) together with the relationships between cooling rate, viscosity at the glass transition and relaxation time (Dingwell and Webb, 1990).

We have also used Eq. (2) to calculate T_g for each of the anhydrous and hydrous samples using a single viscosity value (η_{T_g}) that best fits the T_g^{peak} and T_g^{onset} for cooling/heating rates of 10 K/min (Fig. 7). The η_{T_g} that best fits T_g^{peak} is $10^{10.68}$ Pa s (standard deviation from 22 data (σ) is $10^{0.31}$ Pa s), while the best fit of T_g^{onset} is provided by a η_{T_g} of $10^{12.29}$ Pa s (σ=$10^{0.75}$ Pa s). Therefore the viscosity at T_g^{onset} is ~1.61 $\log_{10}$ units higher than that at T_g^{peak}. We emphasize here the important observation that there is no correlation between η_{T_g} and either base composition or water content (Fig. 6). The influence of chemistry on the viscosity at the glass transition is entirely taken up in the location of the glass transition temperature itself. Importantly, the addition of significant mole fractions of water to silicate melts does not invalidate the applicability of those equations.

Webb and Knoche (1996) calculated an average viscosity of $10^{11.22}$ Pa s (σ=$10^{0.33}$ Pa s, from 135 data) at T_g^{peak} for cooling/heating rates of 5 K/min for a

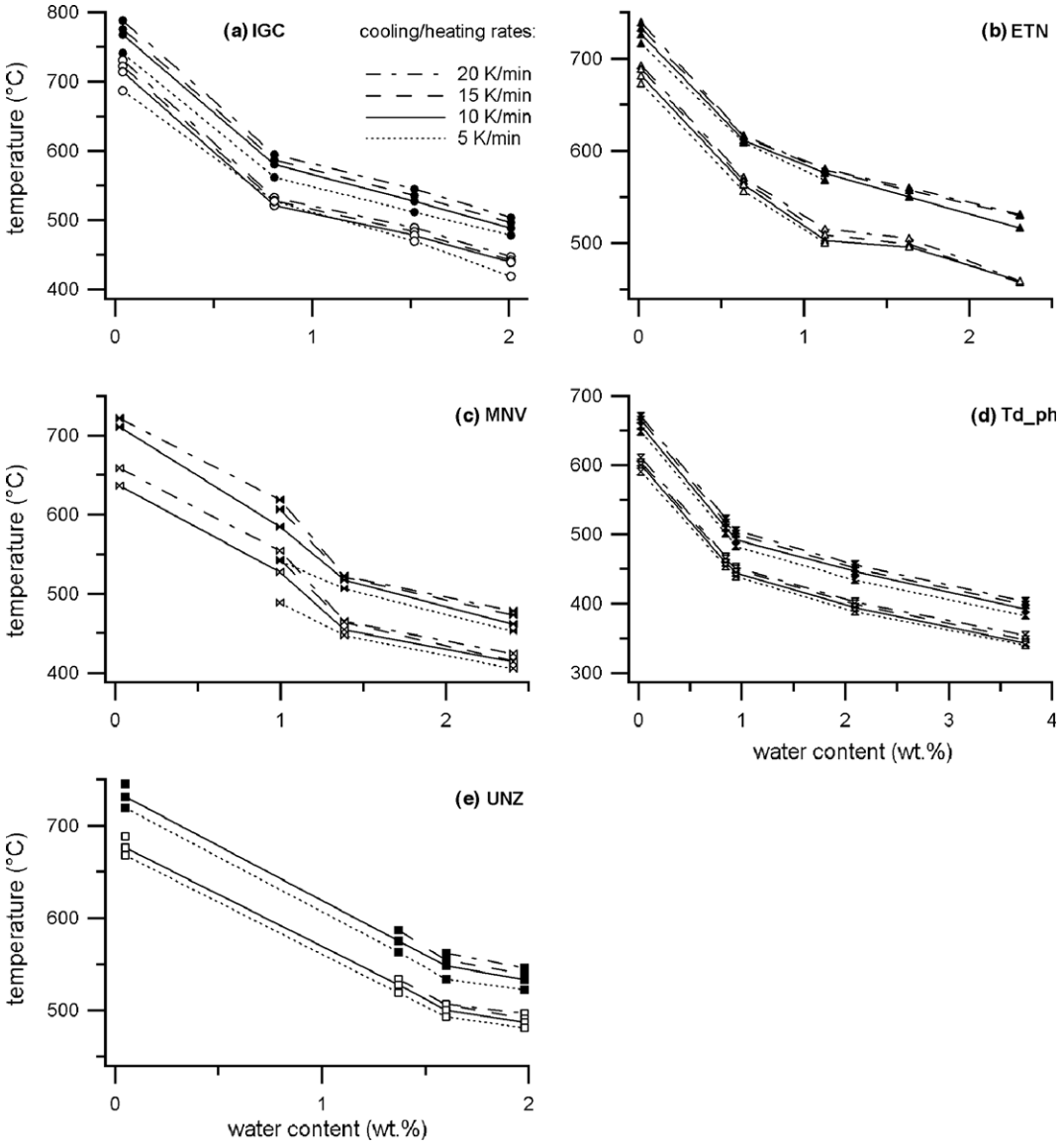

Fig. 4. (a–e) Variation of T_g with water content for each of the compositional suites, showing the effect of thermal history. (a) Campanian ignimbrite trachyte (IGC). (b) Etna basalt (ETN). (c) Monte Nuovo trachyte (MNV). (d) Teide phonolite (Td_ph). (e) Unzen dacite (UNZ). Filled symbols are T_g^{peak} (±1 °C), and open symbols are T_g^{onset} (±2.5 °C).

wide range of dry silicate melt compositions (50 to 85 mol% SiO_2). Our T_g^{peak} data defined using cooling/heating rates of 5 K/min are best reproduced with a η_{T_g} of $10^{11.09}$ Pa s (σ=$10^{0.34}$ Pa s, from 19 data). These values agree within error, and appear to confirm that viscosity at T_g is independent of composition (including water content). However, the value calculated from our dataset for 5 K/min is ~0.41 $\log_{10}$ units higher than the viscosity at T_g^{peak} defined using cooling/heating rates of 10 K/min.

4.4. Relaxation times at the minimum welding temperature

Viewed simply, the total time taken for dense welding is the sum of the time for sintering and

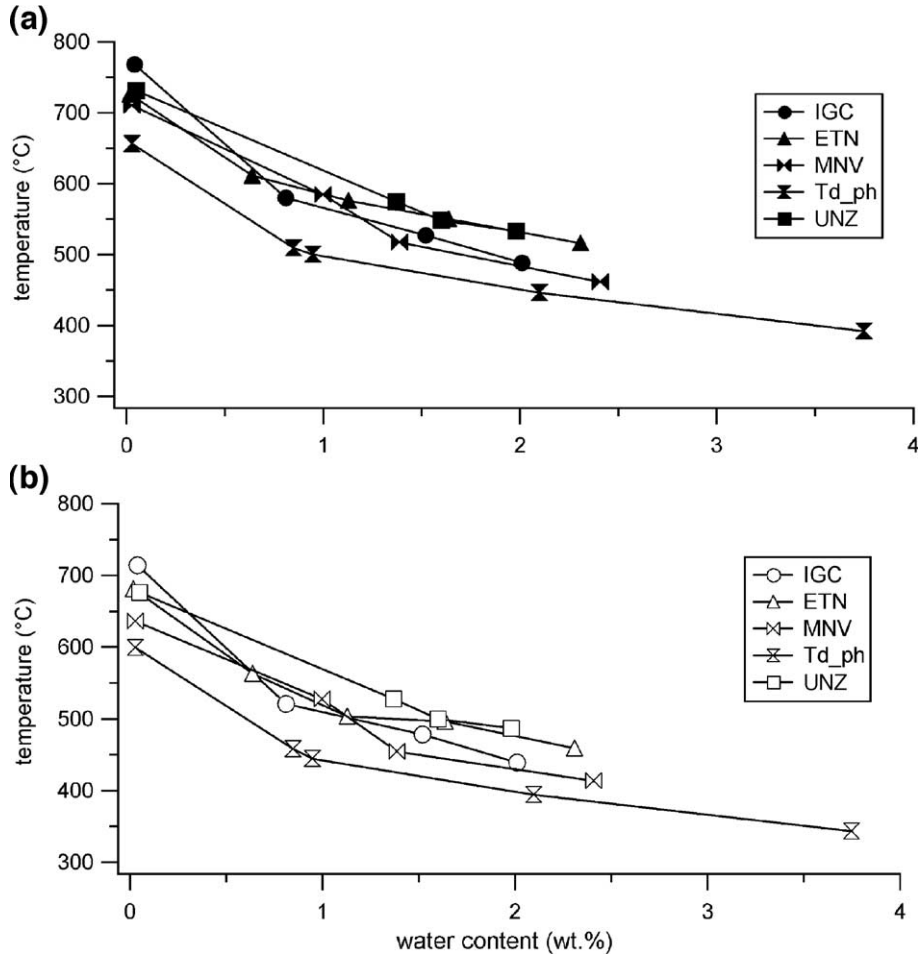

Fig. 5. (a–b) Variation of (a) T_g^{peak} and (b) T_g^{onset} with cooling/heating rates of 10 K/min as a function of water content for each compositional suite.

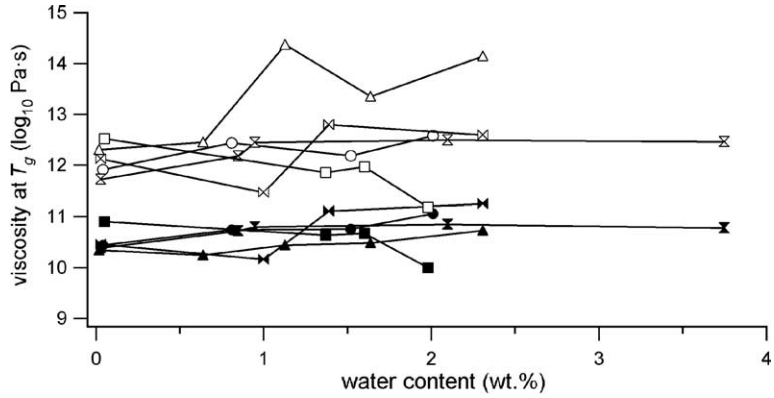

Fig. 6. Viscosities calculated at T_g^{peak} and T_g^{onset} defined with cooling/heating rates of 10 K/min using Eq. (2) as a function of water content for each compositional suite. Symbols as in Fig. 5.

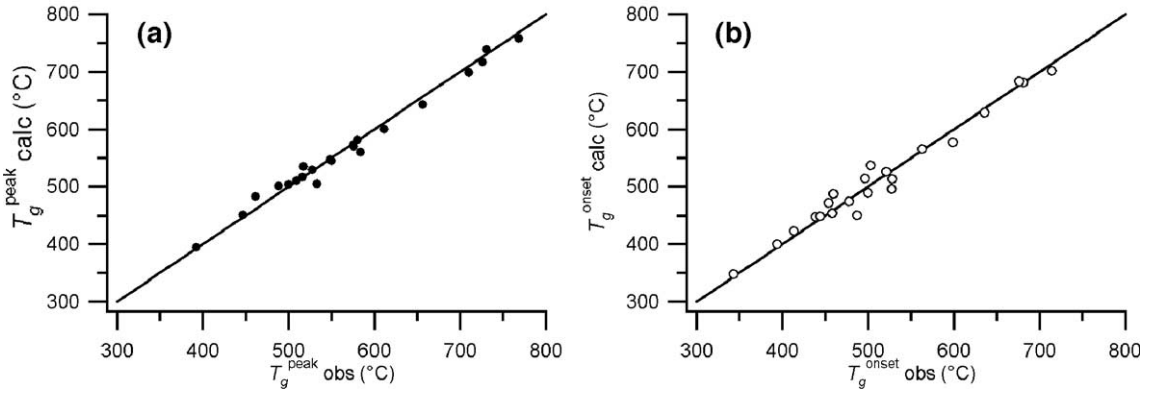

Fig. 7. T_g (T_g calc) obtained from Eq. (2) using a single viscosity value (η_{T_g}) compared with the values observed for (a) T_g^{peak} and (b) T_g^{onset} (T_g obs) at cooling/heating rates of 10 K/min. In each case the line shows where T_g calc=T_g obs. The T_g^{peak} data is best reproduced with a η_{T_g} of $10^{10.68}$ Pa s (σ=$10^{0.31}$ Pa s), while the T_g^{onset} data is best reproduced with a η_{T_g} of $10^{12.29}$ Pa s (σ=$10^{0.75}$ Pa s).

viscous deformation to occur (Tuffen et al., 2003). The relaxation time at the glass transition can provide an estimate of the minimum time required for welding at a given strain rate within the deposit. Therefore, η_{T_g} values are used in Eq. (1) to calculate the relaxation time of the glass at T_g. This provides a scaling for the time required for glass to weld at the minimum welding temperature under viscous deformation for a given loading history in pyroclastic deposits. Assuming cooling/heating rates of 10 K/min and a G_∞ value of 10^{10} Pa (Dingwell and Webb, 1990) the relaxation time at T_g^{peak} is 5 s, while at T_g^{onset} it is 195 s. However, there is a degree of uncertainty in G_∞, with Webb and Knoche (1996) stating that it varies from $10^{9.70}$ to $10^{10.54}$ Pa, depending on composition (and temperature). Together with the standard deviations of the η_{T_g} values, this leads to an overall range in relaxation times from less than 1 to 19 s at T_g^{peak} and 10 to 2165 s at T_g^{onset}. Higher and lower cooling/heating rates result in faster and slower relaxation times at T_g respectively, because the faster the cooling/heating rates the higher T_g. Across the range of experimental heating/cooling rates used in this study (1 to 20 K/min) the variation in relaxation times is within the same order of magnitude. However, for example, in spatter-fed phonolite flows at Teide, Tenerife, Gottsmann and Dingwell (2001) determined cooling rates as slow as 0.0029 K/min. By extrapolating T_g for the Td_ph suite to such a slow cooling rate using the Arrhenian relationship given by Gottsmann et al. (2002) we obtain T_g^{peak} decreasing with water content from 539 to 289 °C and T_g^{onset} decreasing from 512 to 268 °C. Using these T_g we are able to estimate relaxation times of 82 min to 37 h at T_g^{peak}, and 8 h to 7 days at T_g^{onset} at this cooling rate, the range due to uncertainties in G_∞ and η_{T_g} values.

However, these times refer only to homogeneous glasses and do not include the possible effects that crystals and/or bubbles and load pressure have on the relaxation time. Crystals and bubbles may introduce yield strengths, which will lengthen the time required for the deposited material to collapse and weld (Miller and Riehle, 1994; Riehle et al., 1995; Russell and Quane, 2005—this issue), while higher load pressures will accelerate welding processes (Riehle et al., 1995).

5. Conclusions

This study presents the first successful determinations of glass transition temperatures (T_g) in natural hydrous silicate liquids. Our essential findings are as follows. Firstly, water, particularly the first 1 wt.%, has a strong influence on the T_g of the compositions investigated here. Secondly, composition affects T_g, with the lowest temperatures measured in the peralkaline phonolite from Teide, Tenerife (Td_ph). Thirdly, viscosity at T_g is independent of water content and composition. However, T_g of a sample depends on the cooling history, the heating rate at which the measurement is performed and the way in which T_g is defined.

As a result, the value of viscosity at T_g also depends on these factors. An average viscosity value at T_g calculated from all the natural samples in this study, defined in exactly the same way as in Webb and Knoche (1996), is consistent with their value obtained from a number of synthetic samples. Thus the equations relating cooling rate, viscosity at the glass transition and relaxation time developed for anhydrous melts are equally well applicable to natural hydrous melts.

In general, this means that for the case of deposits where welding is controlled by viscous deformation of the glassy phase, the glass transition temperature can serve as a scaling temperature for the ability of volcanic deposits to weld under given thermal histories and loading histories. The parameterisation of the glass transition temperature provided here allows quantitative estimates of the minimum temperatures attendant on welding of glassy volcanic deposits and how these temperatures vary with water content.

Finally, the glass transition temperatures provide a lower limit for the emplacement temperatures of pyroclastic density currents that give rise to densely welded deposits. This may be of interest in numerical simulation studies that assess volcanic hazards.

Acknowledgements

This work was supported by the GNV (Italian National Group of Volcanology) project-27, the IQN (International Quality Network)-Georisk DAAD project, the Volcano Dynamics EU Research Training Network (HPRN-CT-2000-00060) and DFG Unzen Drilling Project Di 431/20-2. We thank Dr. H. Behrens of the Institute of Mineralogy-Hannover (IMH) for facilitating the KFT measurements. The manuscript has benefited from critical discussions with C. Romano, H. Tuffen, L. Pioli and J.K. Russell and constructive reviews by A. Whittington and I. Skilling.

References

Biewirth, P.N., 1982. Experimental welding of volcanic ash. MSc thesis, Monash University.

Boyd, F.R., Kennedy, G.C., 1951. Some experiments and calculations relating to the origin of welded tuffs. Trans. Am. Geophys. Union 32, 327–328.

Branney, M.J., Kokelaar, B.P., McConnell, B.J., 1992. The Bad Step Tuff: a lava-like rheomorphic ignimbrite in a calc-alkaline piecemeal caldera, English Lake District. Bull. Volcanol. 54, 187–199.

Dingwell, D.B., 1991. Redox viscometry of some iron-bearing silicate liquids. Am. Mineral. 76, 1560–1562.

Dingwell, D.B., 1996. Volcanic dilemma: flow or blow? Science 273, 1054–1055.

Dingwell, D.B., Virgo, D., 1988. Melt viscosities in the Na_2O–FeO–Fe_2O_3–SiO_2 system and factors controlling the relative viscosities of fully polymerized silicate melts. Geochim. Cosmochim. Acta 52, 395–403.

Dingwell, D.B., Webb, S.L., 1989. Structural relaxation in silicate melts and non-Newtonian melt rheology in igneous processes. Phys. Chem. Miner. 16, 508–516.

Dingwell, D.B., Webb, S.L., 1990. Relaxations in silicate melts. Eur. J. Mineral. 2, 427–449.

Dingwell, D.B., Courtial, P., Giordano, D., Nichols, A.R.L., 2004. Viscosity of peridotite liquid. Earth Planet. Sci. Lett. 226, 127–138.

Friedman, I., Long, W., Smith, R.L., 1963. Viscosity and water contents of rhyolitic glass. J. Geophys. Res. 68, 6523–6535.

Giordano, D., Dingwell, D.B., 2003a. Viscosity of hydrous Etna basalt: implications for Plinian-style basaltic eruptions. Bull. Volcanol. 65, 8–14.

Giordano, D., Dingwell, D.B., 2003b. Non-Arrhenian multicomponent melt viscosity: a model. Earth Planet. Sci. Lett. 208, 337–349.

Giordano, D., Dingwell, D.B., 2003c. The kinetic fragility of natural silicate liquids. J. Phys., Condens. Matter 15, S945–S954.

Giordano, D., Dingwell, D.B., Romano, C., 2000. Viscosity of a Teide phonolite in the welding interval. J. Volcanol. Geotherm. Res. 103, 239–245.

Giordano, D., Romano, C., Papale, P., Dingwell, D.B., 2004. The viscosity of trachytes, and comparison with basalts, phonolites, and rhyolites. Chem. Geol. 213, 49–61.

Gottsmann, J., Dingwell, D.B., 2001. Cooling dynamics of spatter-fed phonolite obsidian flows on Tenerife, Canary Islands. J. Volcanol. Geotherm. Res. 105, 323–342.

Gottsmann, J., Dingwell, D.B., 2002. The thermal history of a spatter-fed lava flow: the 8-ka pantellerite flow on Major Island, New Zealand. Bull. Volcanol. 64, 410–422.

Gottsmann, J., Giordano, D., Dingwell, D.B., 2002. Predicting shear viscosity at the glass transition during volcanic processes: a calorimetric calibration. Earth Planet. Sci. Lett. 198, 417–427.

Hess, K.-U., Dingwell, D.B., 1996. Viscosities of hydrous leucogranitic melts: a non-Arrhenian model. Am. Mineral. 81, 1297–1300.

Hess, K.-U., Dingwell, D.B., Gennaro, C., Mincione, V., 2001. Viscosity–temperature behaviour of dry melts in the Qz–Ab–Or system. Chem. Geol. 174, 133–142.

Kamata, H., Suzuki-Kamata, K., Bacon, C.R., 1993. Deformation of the Wineglass welded Tuff and the timing of caldera

collapse at Crater lake, Oregon. J. Volcanol. Geotherm. Res. 56, 253–266.
Maxwell, J.C., 1867. On the dynamical theory of glasses. Philos. Trans. R. Soc. Lond. Ser. A: Math. Phys. Sci. 157, 49–88.
Miller, T.F., Riehle, J.R., 1994. A users manual for Ashpac. Technical report No. TR 94-14, Penn. State University.
Moynihan, C.T., 1995. Structural relaxation in the glass transition. In: Stebbins, J.F., McMillan, P.F., Dingwell, D.B. (Eds.), Structure, dynamics and properties of silicate melts. Reviews in Mineralogy, vol. 32. Mineralogical Society of America, Washington, D.C., pp. 1–19.
Ohlhorst, S., Behrens, H., Holtz, F., 2001. Compositional dependence of molar absorptivities of near-infrared OH- and H_2O bands in rhyolitic to basaltic glasses. Chem. Geol. 174, 5–20.
Ragan, D.M., Sheridan, M.F., 1972. Compaction of the Bishop Tuff, California. Geol. Soc. Am. Bull. 83, 95–106.
Richet, P., Lejeune, A.-M., Holtz, F., Roux, J., 1996. Water and the viscosity of andesite melts. Chem. Geol. 128, 185–197.
Riehle, J.R., Miller, T.F., Bailey, R.A., 1995. Cooling, degassing and compaction of rhyolitic ash flow tuffs: a computational model. Bull. Volcanol. 57, 319–336.
Romano, C., Giordano, D., Papale, P., Mincione, V., Dingwell, D.B., Rosi, M., 2003. The dry and hydrous viscosities of alkaline melts from Vesuvius and Phlegrean Fields. Chem. Geol. 202, 23–38.
Ross, C.S., Smith, R.L., 1961. Ash-flow tuffs; their origin, geologic relations, and identification. U.S. Geol. Surv. Prof. Pap., Report: P 0366, 81 pp.
Russell, J.K., Quane, S.L., 2005. Rheology of welding: inversion of field constraints. J. Volcanol. Geotherm. Res 142, 173–191 (this issue).
Scherer, G.W., 1984. Use of the Adam–Gibbs equation in the analysis of structural relaxation. J. Am. Ceram. Soc. 67, 504–511.
Schmincke, H.U., 1974. Volcanological aspects of peralkaline silicic welded ash-flow tuffs. Bull. Volcanol. 38, 594–636.
Smith, R.L., 1960a. Ash flows. Geol. Soc. Am. Bull. 71, 795–842.
Smith, R.L., 1960b. Zones and zonal variations in welded ash fall. U. S. Geol. Surv. Prof. Pap. 354-F, 149–159.
Sparks, R.S.J., Wright, J.V., 1979. Welded air-fall tuffs. Spec. Publ. Geol. Soc. Am. 180, 155–166.
Sparks, R.S.J., Tait, S.R., Yanev, Y., 1999. Dense welding caused by volatile resorption. J. Geol. Soc. (Lond.) 156, 217–225.
Stevenson, R.J., Dingwell, D.B., Webb, S.L., Bagdassarov, N.S., 1995. The equivalence of enthalpy and shear stress relaxation in rhyolitic obsidian and quantification of the liquid–glass transition in volcanic processes. J. Volcanol. Geotherm. Res. 68, 297–306.
Tuffen, H., Dingwell, D.B., Pinkerton, H., 2003. Repeated fracture and healing of silicic magma generate flow banding and earthquakes? Geology 31, 1089–1092.
Webb, S.L., Knoche, R., 1996. The glass-transition, structural relaxation and shear viscosity of silicate melts. Chem. Geol. 128, 165–183.
Whittington, A., Richet, P., Linard, Y., Holtz, F., 2000. Water and the viscosity of depolymerized aluminosilicate melts. Geochim. Cosmochim. Acta 64, 3725–3736.
Whittington, A., Richet, P., Linard, Y., Holtz, F., 2001. The viscosity of hydrous phonolites and trachytes. Chem. Geol. 174, 209–223.
Wilding, M., Webb, S.L., Dingwell, D.B., 1995. Evaluation of a relaxation geospeedometer for volcanic glasses. Chem. Geol. 125, 137–148.
Wilding, M., Webb, S.L., Dingwell, D.B., Ablay, G., Marti, J., 1996. Cooling variation in natural volcanic glasses from Tenerife, Canary Islands. Contrib. Mineral. Petrol. 125, 151–160.
Wilding, M., Dingwell, D.B., Batiza, R., Wilson, L., 2000. Cooling rates of hyaloclastites: applications of relaxation geospeedometry to undersea volcanic deposits. Bull. Volcanol. 61, 527–536.